substitution. The energetic cost of deformation and the choice of the substituents are indicated by the present ab initio calculations. Of the six ZH_4 molecules studied, CH_4 requires the largest energy for planarization; the corresponding energy for NH_4^+, BH_4^-, and PH_4^+ is also considerable. Planarization is indicated to be relatively easy for AlH_4^- and, to a lesser extent, for SiH_4. The planar–tetrahedral energy difference is inversely related to the Z–H bond strength.

An orbital isomerism is exhibited by the planar forms. The species with more electronegative central atoms, CH_4 and NH_4^+, have π-type HOMOs. The other ZH_4 molecules prefer δ-type HOMOs. The choice of the electronic configuration is determined by the central atom electronegativity. As a result, triplet states lie considerably higher in energy, with the possible exception of planar BH_4^-. The electronic structural dichotomy has interesting consequences. The lumomer with the π-type HOMO pyramidalizes readily without activation. The δ lumomer resists this distortion. The symmetry of the HOMO also determines the kind of substituents needed for stabilization. The π lumomers are stabilized by π-acceptor, σ-donor groups, for example, electropositive substituents. The δ lumomers require π-donor, σ-acceptor groups like OR, NR_2, and F for stabilization. Silanes and alanes with this substitution pattern are more easily studied experimentally. Structural investigations to test our conclusions would be of interest.

Acknowledgments. This work was facilitated by a NATO grant and by the Fonds der Chemischen Industrie through support and a Liebig Stipendium (to E.-U.W). The Regionales Rechenzentrum, Erlangen, provided assistance. We thank Professor J. A. Pople and his associates for the development of the Gaussian series of programs which enabled this work to be carried out.

References and Notes

(1) (a) Department of Chemistry, Rutgers, The State University, New Brunswick, N.J. 08903. (b) Lederle Laboratories, Pearl River, N.Y. 10965.
(2) Gimarc, B. M. *Acc. Chem. Res.* **1974**, *7*, 384. Gimarc, B. M. "Molecular Structure and Bonding—The Qualitative Molecular Orbital Approach"; Academic Press: New York, 1979.
(3) (a) Collins, J. B.; Dill, J. D.; Jemmis, E. D.; Apeloig, Y.; Schleyer, P. v. R.; Seeger, R.; Pople, J. A. *J. Am. Chem. Soc.* **1976**, *98*, 5419, and references cited therein. (b) Krogh-Jesperen, K.; Cremer, D.; Poppinger, D.; Pople, J. A.; Schleyer, P. v. R.; Chandrasekhar, J. *Ibid.*, **1979**, *101*, 4843. (c) Cotton, F. A.; Millar, M. *Ibid.* **1977**, *99*, 7886.
(4) (a) Lathan, W. A.; Hehre, W. J.; Curtiss, L. A.; Pople, J. A. *J. Am. Chem. Soc.* **1971**, *93*, 6377. (b) Minkin, V. I.; Minyaev, R. M. *Zh. Obshch. Khim.* **1979**, *15*, 225. (c) Meyer, H.; Nagorsen, G. *Angew. Chem., Int. Ed. Engl.*, **1979**, *18*, 551. (d) Würthwein, E.-U.; Schleyer, P. v. R. *Ibid.*, **1979**, *18*, 553.
(5) All SCF calculations were performed using the GAUSSIAN 76 series of programs: Binkley, J. S.; Whiteside, R. A.; Hariharan, P. C.; Seeger, R.; Pople, J. A.; Hehre, W. J.; Newton, M. D. Program No. 368, Quantum Chemistry Program Exchange, Indiana University, Bloomington, Ind.
(6) Hariharan, P. C.; Pople, J. A. *Theor. Chim. Acta* **1973**, *28*, 213.
(7) Collins, J. B.; Schleyer, P. v. R.; Binkley, J. S.; Pople, J. A. *J. Chem. Phys.* **1976**, *64*, 5142.
(8) (a) Roothaan, C. C. J. *Rev. Mod. Phys.* **1951**, *23*, 69. (b) Pople, J. A.; Nesbet, R. K. *J. Chem. Phys.* **1954**, *22*, 571.
(9) Binkley, J. S.; Pople, J. A. *Int. J. Quantum Chem., Symp.* **1975**, *9*, 229.
(10) Mulliken, R. S. *J. Chem. Phys.* **1955**, *23*, 1833, 1841, 2338, 2343.
(11) Hehre, W. J.; Stewart, R. F.; Pople, J. A. *J. Chem. Phys.* **1969**, *51*, 2657.
(12) Dewar, M. J. S.; Kirschner, S.; Kollmar, H. W. *J. Am. Chem. Soc.* **1974**, *96*, 5240.
(13) The singlet–triplet energy differences for CH_2 are calculated to be 30.8 (6-31G*//6-31G*) and 20.9 kcal/mol (MP2/6-31G*). Higher levels of theory predict a value of around 11 kcal/mol.[16] See: De Frees, D. J.; Levi, B. A.; Pollack, S. K.; Hehre, W. J.; Binkley, J. S.; Pople, J. A., submitted for publication in *J. Chem. Phys.*
(14) Jemmis, E. D.; Kos, A., unpublished work.
(15) Würthwein, E.-U., unpublished work.
(16) (a) Hay, P. J.; Hunt, U. J.; Goddard III, W. A. *Chem. Phys. Lett.* **1972**, *13*, 30. (b) Staemmler, V. *Theor. Chim. Acta* **1973**, *31*, 49. (c) *Ibid.* **1974**, *35*, 309. (d) Lucchese, R. R.; Schaefer III, H. F. *J. Am. Chem. Soc.* **1977**, *99*, 6765. (e) Roos, B. O.; Siegbahn, P. M. *Ibid.* **1977**, *99*, 7716. (f) Gervy, D.; Verhaegen, G. *Int. J. Quantum Chem.* **1977**, *12*, 115. (g) Harding, L. B.; Goodard III, W. A. *J. Chem. Phys.* **1977**, *67*, 1777. (h) Bauschlicher, Jr., C. W.; Shavitt, I. *J. Am. Chem. Soc.* **1978**, *100*, 739. (i) Shih, S.-K.; Peyerimhoff, S. D.; Buenker, R. J.; Peric, M. *Chem. Phys. Lett.* **1978**, *55*, 217. (j) Also see Lengel, R. K.; Zare, R. N. *J. Am. Chem. Soc.* **1978**, *100*, 7495.

An MO Study on the Structure and the Stability of the $CH_5^+(CH_4)_n$ Cluster (n = 0, 1, 2, and 3)

Shinichi Yamabe,*[1a] Yoshihiro Osamura,[1b] and Tsutomu Minato[1c]

Contribution from the Department of Chemistry, Nara University of Education, Takabatake-cho, Nara 630, Japan, the Department of Chemistry, Faculty of Science, Osaka City University, Sumiyoshi-ku, Osaka 558, Japan, and the Faculty of Engineering, Kyoto University, Sakyo-ku, Kyoto 606, Japan.
Received October 4, 1979

Abstract: An ab initio MO calculation is made for the $CH_5^+(CH_4)_n$ (n = 0, 1, 2, and 3) system with the 4-31G basis set. As a result of the geometry optimization, the first and the second CH_4's attack two elongated C–H bonds successively and the third CH_4 attacks the C–H bond of the methyl group of CH_5^+. The secondary attack of CH_4 ($CH_5^+\cdots CH_4\cdots CH_4$) is found to be energetically unfavorable. The process of clustering, which is influenced by the mutual steric effect of CH_4's, results in the formation of five "satellites" around CH_5^+. The pattern of the electronic interaction involved in the $CH_5^+(CH_4)$ cluster is analyzed by the energy decomposition scheme and configuration analysis. The role of some charge-transfer and polarization interactions on the cluster formation is discussed.

I. Introduction

It is well known that in the gas phase protonated species of nonpolar molecules exist as cluster ions. For H_3^+, the temperature dependence of the equilibria $H_{n-2}^+ + H_2 = H_n^+$ (n = 5, 7, 9, and 11) is measured with the pulsed electron beam mass spectrometer and the structure of the H_n^+ cluster is proposed on the basis of the observed enthalpy changes.[2] According to a recent theoretical calculation, it is affirmed that the process of this clustering is described as the successive attachment of H_2's to three corners of the triangle of H_3^+.[3] Protonated methane, CH_5^+, has also attracted much attention as a "superacid" and some gas-phase experiments have been

0002-7863/80/1502-2268$01.00/0

Table I. Calculated Energies for the Cluster $CH_5^+(CH_4)_n$ with the 4-31 G Basis Set

n	cluster	model	total energy (E_T), au	$\Delta E_{n-1,n}$,[a] kcal/mol	$\Delta H^{expl}_{n-1,n}$,[b] kcal/mol	Figure[c]
	CH_4 [T_d]		−40.139 774			1
0	CH_5^+ [C_s]		−40.327 153	−118	−126	1
1	$CH_5^+(CH_4)$	A	−80.471 908	−3.1 (−4.5)[e]		3
1	$CH_5^+(CH_4)$	B	−80.471 282	−2.7	−7.4	3
1	$CH_5^+(CH_4)$	C	−80.467 845	−0.6		3
2	$CH_5^+(CH_4)_2$	D	−120.61 585	−2.9	−5.9	4
3	$CH_5^+(CH_4)_3$	E	−160.75 747	−1.2[d]	−4.1	5

[a] $\Delta E_{1,2}$ is, for instance, computed by $E_T[CH_5^+(CH_4)_2] - E_T[CH_5^+(CH_4)] - E_T[CH_4]$. [b] Taken from ref 4. [c] Figures in which the optimized geometries are displayed. [d] While the decrease of the calculated stabilization energies is as expected, the large gap between $n = 2$ and $n = 3$ is due to the partial optimization of the $CH_5^+(CH_4)_3$ geometry (only the orientation of the third CH_4 changed). [e] Reference 13.

made, giving the enthalpy changes ($\Delta H_{n-1,n}$) for the process $CH_5^+(CH_4)_{n-1} + CH_4 = CH_5^+(CH_4)_n$ (n = 1-5). The plot of the experimental $\Delta H_{n-1,n}$ vs. n gives some information on the behavior of clustering. There is a large difference between $\Delta H_{1,2}$ and $\Delta H_{2,3}$ and a small one between $\Delta H_{2,3}$ and $\Delta H_{3,4}$, showing that the first incoming CH_4 molecules interact moderately, while the next three molecules participate in the clustering weakly and similarly.[4] Although it is natural that the gradual charge dispersal with the addition of new CH_4 lessens $\Delta H_{n-1,n}$, its change obtained experimentally seems to indicate the characteristic of such cluster formation. Thus, it is tempting to examine theoretically the mode of interaction involved in this gaseous ion and the pattern of charge dispersal when the size of the cluster becomes large. In this work, the possible structure and the stability of the $CH_5^+(CH_4)_n$ cluster are studied with the ab initio MO calculation.

II. Method of Calculation

The electronic structure of $CH_5^+(CH_4)_n$ is obtained with the usual Hartree-Fock SCF MO using the GAUSSIAN 70 program package.[5] The STO-3G minimal basis set is primarily adopted for $CH_5^+(CH_4)$ and $CH_5^+(CH_4)_2$, and it is found that such a small basis set cannot reproduce the stable structure of cluster ions owing to the absence of the widely spread orbitals. In the weakly interacting system, the inclusion of diffused-type orbitals is necessary; otherwise the long-range attractive energy is not obtained in a system without the heteroatoms.[6] Next, the 4-31G basis set is tested and is found to give the attractive potential between CH_5^+ and CH_4. Although this 4-31G basis still seems small in the sense of the accurate energetics, we are obligated to use it owing to the large size of the system. For instance, $CH_5^+(CH_4)_3$ has 70 functions in this basis set. The geometries of CH_5^+, $CH_5^+(CH_4)$, $CH_5^+(CH_4)_2$, and $CH_5^+(CH_4)_3$ are optimized to minimize the total energies for all or partial geometrical parameters and the stabilization energies ($\Delta E_{n-1,n}$) are evaluated for this series of clusters.

III. Result of Optimization

CH_5^+. A rigorous geometry optimization of the protonated methane was made with the near Hartree-Fock limit calculation by Kutzelnigg and his co-workers.[7] Their result shows that the most stable structure has C_s symmetry. Starting from their geometry, it is reoptimized with the 4-31G basis set and its result is shown together with that of CH_4 in Figure 1 and Table I. In this calculation, all the bond lengths (except $r(C_I\text{-}H_d) = r(C_I\text{-}H_e)$) are optimized and it is found that $r(C_I\text{-}H_a)$ is slightly different from $r(C_I\text{-}H_b)$. Here, it is noteworthy that the electron population on H_c, H_d, and H_e is larger than that on H_a and H_b. This difference apparently makes the attack of CH_4 toward the methyl side of CH_5^+ favorable. However, as is shown for the $CH_5^+(CH_4)$ geometry, the clustering toward the $C_I\text{-}H_a$ (or $C_I\text{-}H_b$) bond is energetically more stable. This discrepancy comes from the fact that

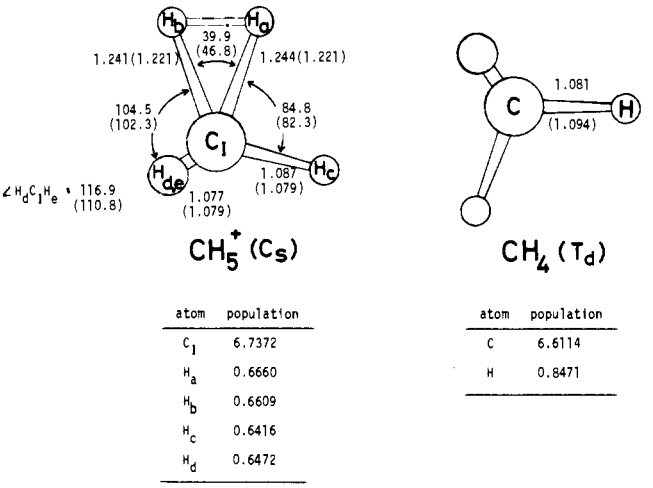

atom	population
C_I	6.7372
H_a	0.6660
H_b	0.6609
H_c	0.6416
H_d	0.6472

atom	population
C	6.6114
H	0.8471

Figure 1. The optimized geometries and the electron population on each atom of CH_5^+ and CH_4 calculated with the 4-31G basis set. The bond length is in angstroms and the angle is in degrees. Angles are measured within a cut plane composed of C_I, H_a, H_b, and H_c atoms. The values in parentheses are those given by Kutzelnigg et al.[7]

the selectivity and the orientation of the attack of CH_4 are determined not by the net charge but by the spatial extension of some low-lying vacant orbitals of CH_5^+. For the discussion of clustering in section IV, the shapes of some important ("frontier") MOs of CH_5^+ and CH_4 are schematically drawn and are displayed in Figure 2.[8]

$CH_5^+(CH_4)$. There are various possibilities for CH_4 to attack CH_5^+ which are exhibited below. For all models, the most

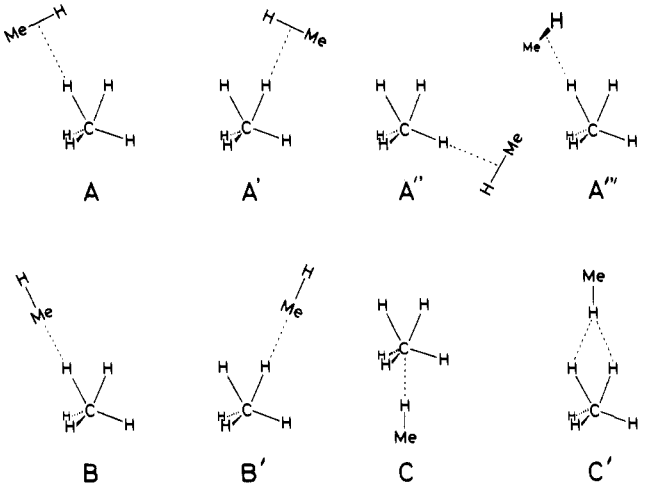

stable structure is sought in terms of the energy optimization. As a result, the geometries of models A, B, and C are found to be stable relative to the infinite separation between CH_5^+ and

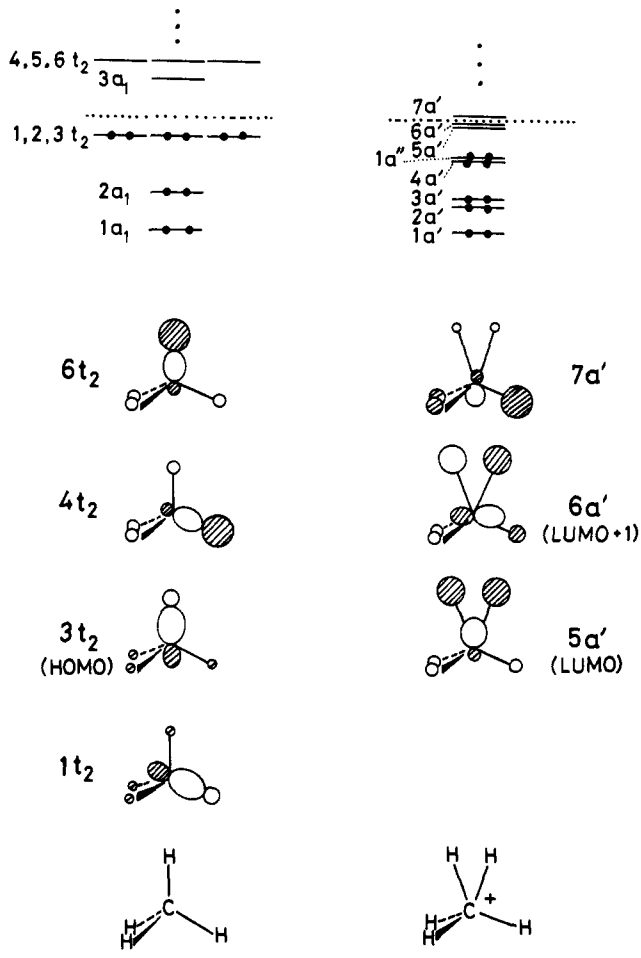

Figure 2. Orbital energies and shapes of MOs of CH_5^+ and CH_4.

CH_4 and are exhibited in Figure 3. Other models may be ruled out owing to the absence of energy minima. In models A and B, CH_4 approaches the C_I–H_b bond of CH_5^+, whereas in model C, CH_4 attacks the methyl side of CH_5^+. The geometries of CH_5^+ and CH_4 in the $CH_5^+(CH_4)$ cluster are not so different from those in their isolated state given in Figure 1. When E_T's displayed in Table I are compared, model A is found to be most stable. However, the geometry of model A is easily interchangeable with that of model B through the following slight movement of CH_4 and they are essentially

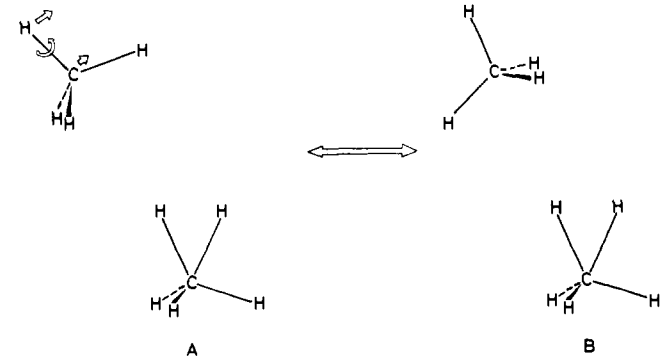

indistinguishable. In fact, the difference of their E_T's is too small to be physically meaningful. The detailed analysis for this cluster will be given in the next section.

$CH_5^+(CH_4)_2$. In view of the most stable geometry of $CH_5^+(CH_4)$, the structure of $CH_5^+(CH_4)_2$ is determined similarly and is shown in Figure 4. The geometry of the $CH_5^+(CH_4)$ part is not altered so drastically by the addition of the second CH_4. However, two points should be noted. One is that the geometry is based on model B of $CH_5^+(CH_4)$ rather than model A. The other is the effect of the steric hindrance which makes two CH_4's separate. In model D, once the C_I–H_b bond of CH_5^+ is occupied, that along the C_I–H_a is attacked. An alternative model, $CH_5^+\cdots CH_4\cdots CH_4$, in which the C_{II}–H_f bond of the first CH_4 is attacked by the second CH_4, is unfavorable. This is because the electron-deficient character causing the attractive intermolecular force is not transmitted effectively to the first CH_4.

Table II. Interaction Energy for Three Models of $CH_5^+(CH_4)$ Obtained by the Energy Decomposition Scheme of Kitaura and Morokuma[a]

definition	comment for each term	model A	model B	model C
$\Delta E_{0,1}$	net interaction energy defined in Table I $\Delta E_{0,1} = E_{def} + E_{el}$	−3.131	−2.734	−0.576
E_{def}	destabilization due to the deformation of CH_5^+ and CH_4	0.434	0.905	0.119
E_{el}	total electronic interaction; sum of the following seven terms	−3.564	−3.639	−0.695
ES	electrostatic energy	−2.234	−2.452	0.240
EX	exchange repulsion	5.300	5.874	0.632
pl(CH_5^+)	polarization energy in CH_5^+	−0.006	−0.006	−0.001
pl(CH_4)	polarization energy in CH_4	−2.346	−2.541	−1.064
CT($CH_4 \rightarrow CH_5^+$)	charge-transfer energy	−2.148	−2.202	−0.235
CT($CH_5^+ \rightarrow CH_4$)	back CT energy	−0.121	−0.121	−0.056
MIX	coupling term	−2.009	−2.191	−0.211

[a] All values are in kcal/mol. Negative values correspond to the stabilization of the system.

$CH_5^+(CH_4)_3$. Since the geometries of CH_5^+ and CH_4 are found to be hardly different from those in the cluster and the interaction between $CH_5^+(CH_4)_2$ cluster and CH_4 is weak, the structure of $CH_5^+(CH_4)_3$ may be determined with only the intermolecular $[CH_5^+(CH_4)_2\cdots CH_4]$ distance and the orientation changed. For this system, the most important point is whether the third CH_4 approaches CH_5^+ or CH_4. For each possibility, the stable geometry is sought. As a result of the geometry optimization, the third CH_4 is found to approach the C_I–H_c bond of CH_5^+ (model E in Figure 5 and Table I). However, any orientation of the third CH_4 toward the hydrogen either of the first CH_4 (H_f, H_g) or of the second CH_4 (H_j, H_k) gives no energy minimum. Although the geometry of the cluster is not fully optimized, the present calculation shows the preference of $CH_5^+\cdots(CH_4)_3$ over $CH_5^+\cdots(CH_4)_2\cdots CH_4$.

IV. Discussion of the $CH_5^+(CH_4)$ Cluster

Let us analyze the mode of the interaction involved in $CH_5^+(CH_4)$. The energy decomposition scheme put forth by Kitaura and Morokuma[9] and configuration analysis[10] are the useful tools for this purpose. Table II gives the result of the energy decomposition scheme for three models of $CH_5^+(CH_4)$. In this two-body interacting system, model A gains the largest attractive energy. The fact that a repulsive term, E_{def}, is small (= 0.434 kcal/mol) indicates that drastic geometrical change is not necessary to yield the $CH_5^+(CH_4)$ cluster. The largest term (absolute value) of the electronic component, E_{el}, is found to be EX, which originates from the overlap of the electronic cloud of CH_5^+ with that of CH_4. The superiority of model A over model A‴ is attributed almost completely to the smaller EX. It should be noted that E_{el} is not composed of a particular term but consists of the balance of all small values. This result shows that the electronic interaction is so weak as to be re-

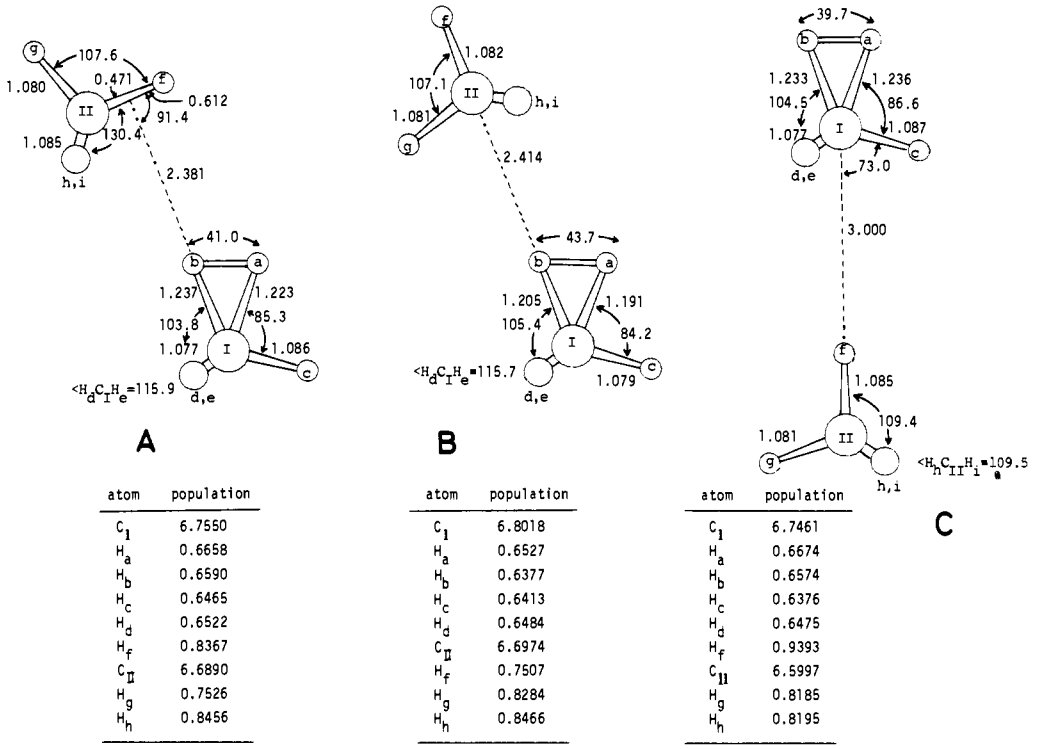

Figure 3. The optimized geometries and the electron population of $CH_5^+(CH_4)$ for three models.

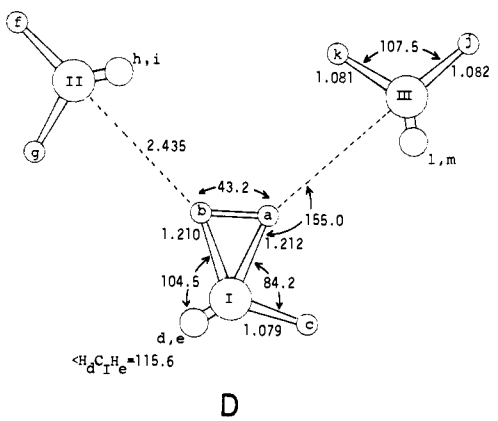

Figure 4. The optimized geometries of $CH_5^+(CH_4)_2$. The intermolecular distance and the orientation of two CH_4's toward CH_5^+ are taken to be equivalent and the $H_b\cdots C_{II}-H_f$ and $H_a\cdots C_{III}-H_j$ are taken to be collinear.

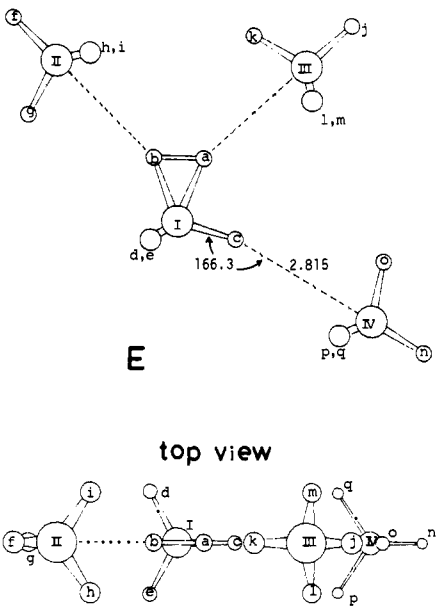

Figure 5. The geometry of $CH_5^+(CH_4)_3$. The structures of $CH_5^+(CH_4)_2$ and the third CH_4 are fixed to those shown in Figures 4 and 1, respectively.

garded as a perturbation and that the "one-term approximation" for $CH_5^+\cdots CH_4$ interaction is not appropriate to describe its origin. Such weakly bonding nature makes any model with significant geometrical rearrangement in the process of clustering improbable. Instead, the stability of the system is obtained by a *gentle* contact of the C–H bond with an electron-deficient C_I-H_b bond. It is obvious that $pl(CH_4)$ is much larger than $pl(CH_5^+)$ and $CT(CH_4\rightarrow CH_5^+)$ is larger than $CT(CH_5^+\rightarrow CH_4)$. The field presented by the CH_5^+ cation gives rise to the polarization of the electron donor, CH_4. When each term of model A is compared with that of model B, E_{def} of the latter is found to be slightly larger than that of the former. This destabilization energy of model B is brought about by the increase of the $\angle H_b\cdots C_{II}-H_g$ angle (i.e., the spreading of the H_3C- "umbrella") due to cluster formation. The instability of model C compared to model A is shown clearly by the smaller E_{el}. The electronic cloud composed of the methyl group of CH_5^+ interferes with the approach of the "electron-rich" C–H bond of CH_4 through the exchange repulsion.

In order to investigate the behavior of the charge redistribution in the $CH_5^+(CH_4)$ cluster formation, configuration analysis is carried out for model A. By the use of this method, the mode of the molecular interaction may be interpreted in terms of the monomer MOs and the wave function of the cluster $[\Psi(A)]$ is described by the sum of various electron configurations:

$$\Psi(A) = 0.975\Psi_0 - 0.051\Psi^{CT}_{3t_2\rightarrow 5a'} + 0.026\Psi^{CT}_{1t_2\rightarrow 5a'} + 0.025\Psi^{CT}_{1t_2\rightarrow 6a'} + 0.016\Psi^{CT}_{2a_1\rightarrow 5a'} - 0.044\Psi^{pl(CH_4)}_{3t_3\rightarrow 6t_2} + 0.017\Psi^{pl(CH_4)}_{3t_2\rightarrow 3a_1} - 0.014\Psi^{pl(CH_4)}_{2t_2\rightarrow 4t_2} + 0.011\Psi^{pl(CH_4)}_{1t_2\rightarrow 6t_2} - 0.010\Psi^{pl(CH_4)}_{3t_2\rightarrow 5t_2} + \ldots \quad (1)$$

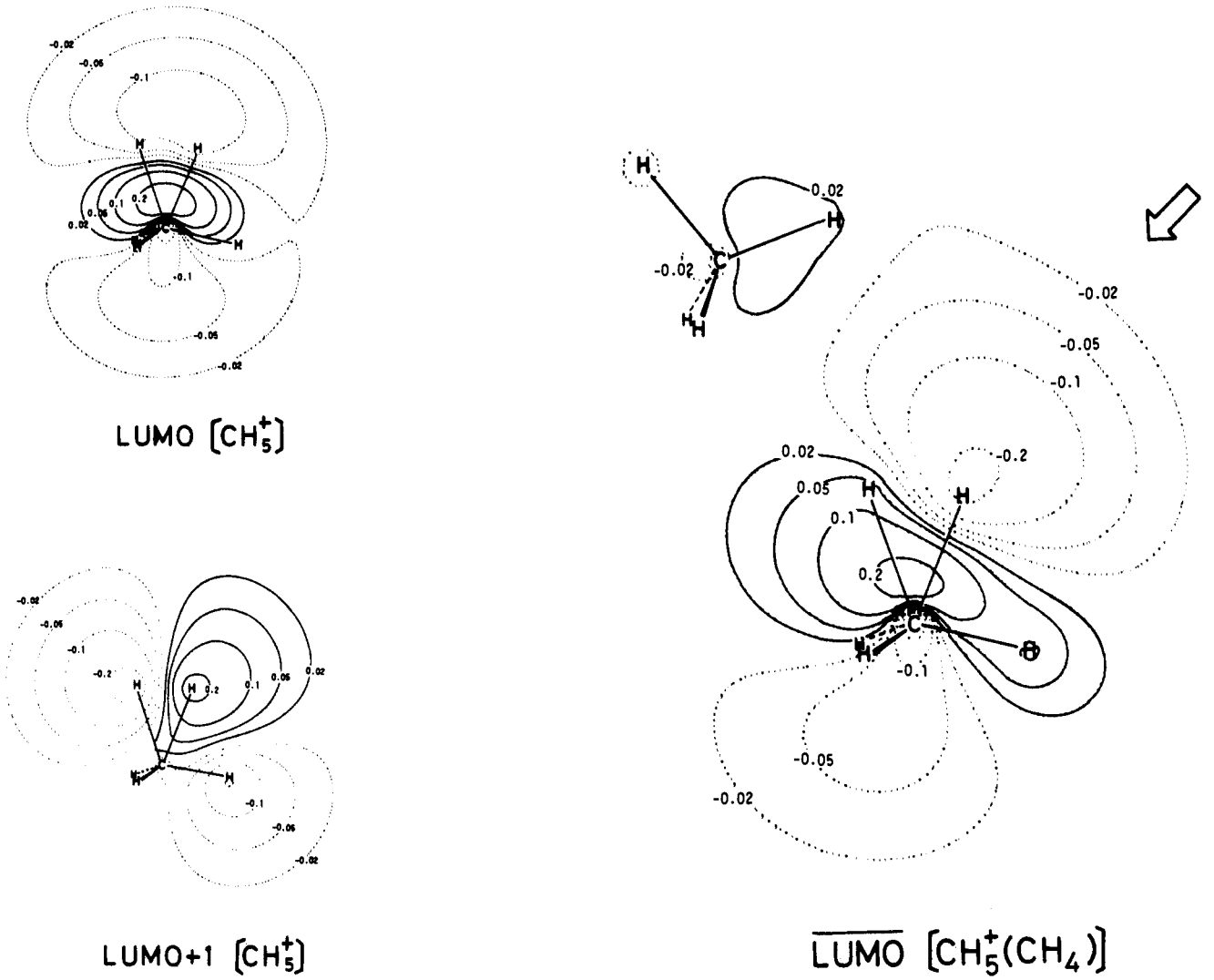

Figure 6. The change of the shape of the dominant unoccupied MOs before and after clustering (model A). The unit of the contour lines is bohr^{-3}. The bold arrow shown in the upper right corner indicates that the direction of the attachment of the second CH_4 coincides with that of the largest extension of the LUMO of $CH_5^+(CH_4)$.

Ψ_0 is the original configuration without any electron jumping (adiabatically interacting state). In eq 1, only major configurations with coefficients of more than 0.01 (absolute value) are shown. Therefore, the small contribution of $\Psi^{\text{back CT}}$ and $\Psi^{\text{pl}(CH_5^+)}$ is omitted in eq 1. Among four CT configurations exhibited in eq 1, the dominant one is $\Psi^{CT}_{3t_2\to 5a'}$, which is composed of the C_{II}–H_f bonding orbital of CH_4 and the LUMO of CH_5^+ localized at the C_I–H_b bond. The most important pl configuration is $\Psi^{\text{pl}(CH_4)}_{3t_2\to 6t_2}$ where $3t_2$ and $6t_2$ have the lobe spreading toward the LUMO of CH_5^+. While the contribution of these electron configurations is expected to cause geometrical distortion at the cluster formation, its degree is calculated to be negligibly small and this result is reflected by the comparable small values of the coefficients attached to CT and pl configurations. In general, when a molecular interaction is strong enough to change the geometry drastically, one particular CT configuration has a remarkably large contribution, corresponding to the fact that the formation of the stable bond is *frontier controlled*. In this weakly bonded cluster, such a particular configuration is absent.

In the previous section, it was found that the first, the second, and the third CH_4's attack the C_I–H_b, C_I–H_a, and C_I–H_c bonds, respectively. This mode of clustering is interpreted in terms of the orbital interaction concept. Although the energy decomposition scheme demonstrates that the effect of the CT interaction is not so remarkably large, it still has an important role of controlling the orientation of clustering. Especially, the spatial extension of some vacant MOs of CH_5^+ which are eager to accept electrons determines the degree of the CT interaction, and then the orientation of CH_4 is affected by the shape of these particular MOs. For the attack of the first CH_4, the LUMO (5a′) and the LUMO + 1 (6a′) of CH_5^+ exhibited in Figure 2 play cooperatively the role of the charge acceptance through $\Psi^{CT}_{3t_2\to 5a'}$ and $\Psi^{CT}_{3t_2\to 6a'}$. Similarly, the attacking site of CH_4 toward $CH_5^+(CH_4)_{n-1}$ ($n \geq 2$) is considered to be in accord with the direction along which its LUMO is localized. Thus, the investigation of orientation of CH_4 is reduced to the analysis of the shape of this particular (frontier) vacant orbital. Let us consider the case of $CH_5^+(CH_4) + CH_4 \rightarrow CH_5^+(CH_4)_2$. The LUMO of $CH_5^+(CH_4)$, $\overline{\text{LUMO}}$, is composed mainly of the HOMO[CH_4], LUMO[CH_5^+], and LUMO + 1[CH_5^+]. The three MOs of $CH_5^+(CH_4)$ ($\overline{\text{HOMO}}$, $\overline{\text{LUMO}}$, and $\overline{\text{LUMO}+1}$) are yielded approximately through the combination of these three MOs. In the framework of such "three-orbital" treatment, the $\overline{\text{LUMO}}$ which is the second orbital of $CH_5^+(CH_4)$ should have a node and be described as $\overline{\text{LUMO}}[CH_5^+(CH_4)] \simeq \text{HOMO}[CH_4] - \text{LUMO}[CH_5^+] + \text{LUMO} + 1[CH_5^+]$. The mode of this MO mixing localizes the $\overline{\text{LUMO}}$ of $CH_5^+(CH_4)$ significantly on the H_a atom of CH_5^+. The validity of this discussion is affirmed by the analysis of the density map of LUMO[CH_5^+], LUMO + 1[CH_5^+], and $\overline{\text{LUMO}}[CH_5^+(CH_4)]$ given in Figure 6. Thus, the addi-

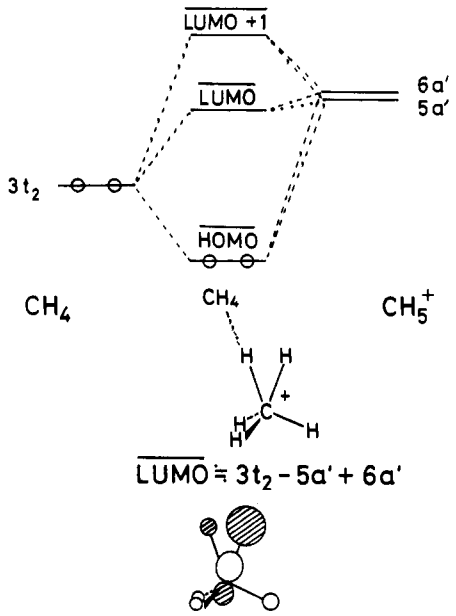

tion of CH_4 to CH_5^+ enlarges the $\overline{\text{LUMO}}$ of $CH_5^+(CH_4)$ at the C_I-H_a region, and there the approach of the second CH_4 becomes welcome. The same discussion of the mode of MO mixing generally holds for the orientation of CH_4 toward $CH_5^+(CH_4)_{n-1}$ (n = 2, 3, 4, and 5). Although the geometries of $CH_5^+(CH_4)_4$ and $CH_5^+(CH_4)_5$ are not traced here, the fourth and the fifth CH_4's are expected reasonably to attack the C_I-H_d and C_I-H_e bonds of CH_5^+, respectively, according to such analysis. The position where the LUMO of $CH_5^+(CH_4)_n$ is localized migrates (C_I-H_b → C_I-H_a → C_I-H_c → C_I-H_d and C_I-H_e) through the addition of CH_4 to $CH_5^+(CH_4)_{n-1}$.

V. Concluding Remarks

In this work, we investigated how CH_4's attack protonated methane. While CH_4's are expected to approach the cationic center of CH_5, the sequence of the attack is determined by the degree of the spatial extension of particular vacant orbitals (LUMO and LUMO + 1) along each C-H bond of CH_5^+. When the first CH_4 is located along a C-H bond, the LUMO of the newly formed cluster, $CH_5^+(CH_4)$, is enlarged at the second C-H bond. Thus, the attachment of the first CH_4 enhances that of the second and more CH_4's, resulting in the five "satellite" molecules around the parent CH_5^+. The secondary attachment, $CH_5^+\cdots CH_4\cdots CH_4$, may be unlikely, because the cationic character of CH_5^+ is not transmitted to the first CH_4. In this respect, the coordination of the sixth CH_4 to $CH_5^+(CH_4)_5$ seems improbable. Also, CH_4's interact with CH_5^+ so weakly that the intermolecular bonds are not regarded as the "bridged three-centered" ones. That is, such degree of interaction belongs to a perturbation and the geometrical deformation is negligibly small. Hiraoka and Kebarle speculated that $CH_5^+(CH_4)_4$ exists as $CH_5^+\cdots(CH_4)_2\cdots(CH_4)_2$ on the basis of a small $\Delta H_{4,5}$ obtained from the van't Hoff plots.[4] However, this model may be ruled out, because the present calculation shows that the secondary attachment does not give enough energetic stability. Instead, when the fifth CH_4 approaches the C_I-H_e bond of CH_5^+, the former molecule will suffer from the steric hindrance presented by three (first, third, and fourth) neighboring CH_4's and its attack may be interfered with to some extent. This interference may be related to the unexpectedly small $\Delta H_{4,5}$. In short, CH_4's approach successively CH_5^+ under the influence of the mutual steric effect. This mode of clustering is schematically sketched in Figure 7.

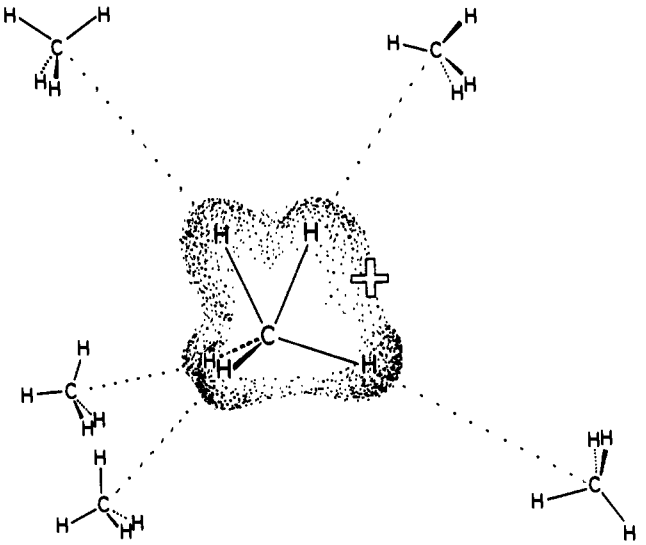

Figure 7. Schematic representation of the mode of the successive attachment of CH_4's to CH_5^+.

Acknowledgment. The authors thank the Institute for Molecular Science (IMS) for the allotment of the CPU time of the HITAC M-180 computer. They would like to express their gratitude to Professor Keiji Morokuma and Dr. Kazuo Kitaura of IMS for permission to use the program of the energy decomposition scheme incorporated in the GAUSSIAN 70 of the Rochester version. The geometries in Figures 1, 3, 4, and 5 are drawn by the use of the plotter program, NAMOD.[14]

References and Notes

(1) (a) Nara University of Education. (b) Osaka City University. (c) Kyoto University.
(2) Hiraoka, K.; Kebarle, P. *J. Chem. Phys.*, **1975**, *62*, 2267.
(3) Yamabe, S.; Hirao, K.; Kitaura, K. *Chem. Phys. Lett.* **1978**, *56*, 546.
(4) Hiraoka, K.; Kebarle, P. *J. Am. Chem. Soc.* **1975**, *97*, 4179.
(5) Hehre, W. J.; Lathan, W. A.; Ditchfield, R.; Newton, M. D.; Pople, J. A. GAUSSIAN 70, Program No. 236, Quantum Chemistry Program Exchange (QCPE), Indiana University, Bloomington, Ind., 1973.
(6) Bertoncini, P.; Wahl, A. C. *Phys. Rev. Lett.* **1970**, *25*, 991.
(7) Dyczmons, V.; Staemmler, V.; Kutzelnigg, W. *Chem. Phys. Lett.* **1970**, *5*, 361.
(8) For the graphic illustration of each MO, see: Jorgensen, W. L.; Salem, L. "The Organic Chemist's Book of Orbitals"; Academic Press: New York, 1973.
(9) Kitaura, K.; Morokuma, K. *Int. J. Quantum Chem.* **1976**, *10*, 325.
(10) Baba, H.; Suzuki, S.; Takemura, T. *J. Chem. Phys.* **1969**, *50*, 2078. Fujimoto, H.; Kato, S.; Yamabe, S.; Fukui, K. *Ibid.* **1974**, *60*, 572.
(11) Fujimoto, H.; Inagaki, S. *J. Am. Chem. Soc.* **1977**, *99*, 7424.
(12) Inagaki, S.; Fujimoto, H.; Fukui, K. *J. Am. Chem. Soc.* **1976**, *98*, 4054.
(13) $\Delta H_{n-1,n}^{\text{expl}}$ should be evaluated ideally by the following equation.
$\Delta H_{n-1,n}^{\text{expl}} = \Delta E_{n-1,n}$ + correlation energy + zero-point vibration energy + temperature correction
Although the latter three terms are not considered here, the effect of the latter two terms seems not so serious. Aside from such strict discussion, $\Delta E_{n-1,n}$ calculated within the 4-31G basis set appears to be somewhat small. Since the interaction between CH_5^+ and CH_4 belongs to a long-range type, the inclusion of p orbitals is expected to change the equilibrium geometry to some extent. To see this effect, the moderately diffused p-type GTO is added to H_b of CH_5^+ and H_f of CH_4. After the optimization of its exponent (=0.56), the intermolecular ($H_b\cdots CH_4$) distance is reoptimized for model A and is found to be shortened (2.38 → 2.22 Å) and $E_{0,1}$ becomes larger {−3.1 (4-31G) → −4.5 kcal/mol (4-31G + p)}. Thus, to cover the gap between $\Delta E_{n-1,n}$ and $\Delta H_{n-1,n}^{\text{expl}}$, it seems important that the correlation energy (in particular the dispersion energy) is estimated with such p orbitals.
(14) Beppu, Y. *QCPE* **1979**, *370*, 11.